USE OF ACCELERATORS TO INVESTIGATE RADIATION DAMAGE, RANGE DISTRIBUTION AND SITE LOCATION OF INERT GASES AND HYDROGEN IN MATERIALS AFTER IMPLANTATION AND ANNEALING

G. D. Tolstolutskaya, I. E. Kopanetz, I. M. Neklyudov

National Science Center "Kharkov Institute of Physics and Technology"
1, Academicheskaya str., 61108 Kharkov, Ukraine, g.d.t@kipt.kharkov.ua

The equipment and parameters of measuring system "ESU-2" are described. Measuring system allow to use the sets of the ion beam analysis techniques including Rutherford backscattering spectroscopy (RBS), channeling, nuclear reaction analysis (NRA). The ion beam technique and methodologies for the analysis of experimental data provide a comprehensive tool for studying crystal defects.

The present paper discusses the application of this tool in the complex investigation of displacement damage and detailed depth profiling of damage and impurity atoms under irradiation of targets in wide range of doses and energies of heavy particles and deuterium. The deuterium-depth profiles were determined by measuring either the α particles or the protons from the ^{3}He-excited nuclear reaction D(^{3}He,α)p. Particular attention is given to the principles of determination the truthful depth profile.

I. INTRODUCTION

Recent efforts on radiation damage study have been making remarkable progresses still it is a long way to establish clear understanding about the material behaviors in fission and fusion environment. Under this situation, charged particle-materials interaction research using the accelerators has to be responsible for contributing to advanced energy materials R & D.

The interactions of hydrogen and helium with defects in solids play an important role for the mechanical behavior of various materials. Hydrogen and helium atoms are generated by nuclear transmutation in fusion and fission reactors, spallation neutron sources and high energy charged particle environments. Garner and coworkers have recently shown that in fission reactors rather high concentrations of hydrogen can accumulate in stainless steels [1]. The retention and accumulation of hydrogen in irradiated stainless steels is most likely caused by the presence of high concentrations of microstructural trapping sites. It is assumed that helium bubbles and voids were the operating traps [2]. On the other hand, the elastic fields around defect clusters are considered by some researchers as the trap for retaining hydrogen [3]. The additional experiments are now in progress to resolve some of these questions.

In the present work, the measuring system "ESU-2" is used for study the retention, accumulation and distribution of hydrogen (deuterium) and displacement damage production under high energy heavy particles (He^+, Ar^+, Kr^+, Xe^+) irradiation. In this manner we have attempted to simulate the displacement damage produced by high energy neutrons. The distribution profiles of damage and impurity atoms under irradiation of targets in wide range of doses (0…100 dpa) and energies of heavy particles (200…1000 keV) were investigated. The crystal structure perfection, the type and number of defects, their depth distribution in near-surface layers, the location of impurity atoms and defects in elementary cell were examined.

II. THE EQUIPMENT AND PARAMETERS OF MEASURING SYSTEM "ESU-2"

The experimental equipment consists of the compact electrostatic accelerator designated "ESU-2 MeV", mass-separator, assembly "Implantator", chambers for irradiation of targets and measurements using the methods of Rutherford backscattering, channeling and nuclear reactions (Fig. 1).

The parameters of measuring system "ESU-2" are: the range of continuously regulated beam energy is 200-1600 keV, (using double-charged ions, we are able to increase the ions energy up to 3.2 MeV); energy stability 0.1 %, maximum of beam current 10 mkA; the kind of accelerated ions - inert from He to Xe, chemically active from hydrogen to nitrogen; the service life not less 4000 hours/year without preventive maintenance.

II.A. Electrostatic accelerator

The original accelerator "ESU-2 MeV" was worked out and created in NSC KIPT. Electrostatic belt generator operating in compressed gas serves as the voltage source.

Generator is situated inside the steel tank. Internal diameter of tank cylinder part is 900 mm, the total height of tank - 1860 mm. Diameter of tank bottom is 680 mm.

Generation insulation column is assembled from 63 equipotential disks and its total height is 1050 mm. The disk construction gives the possibility to insert the belt-charge carrier into the system of its shielding without disassembly of ring elements. This allows to mount the infinite (closed) belt-charge carrier approximately during 3 hours.

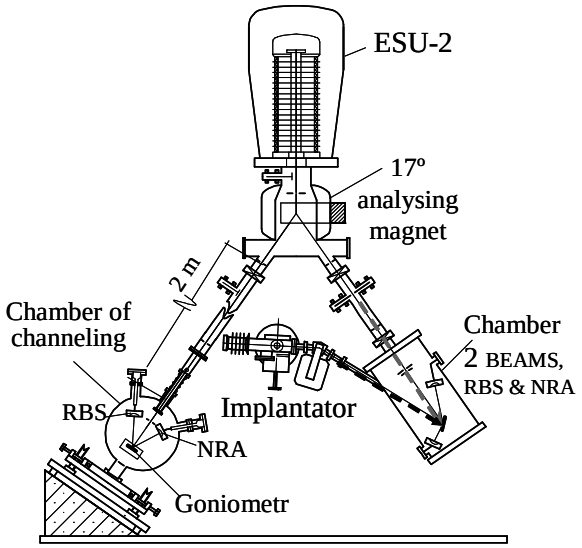

Fig.1. A configuration of measuring system "ESU-2".

II.B. Facility for dual-ion irradiation

Irradiation of specimens with deuterium and helium was carried out using the assembly designated as "Implantator", having an oil-free evacuation system with residual pressure in the target chamber ~$1 \cdot 10^{-4}$ Pa. Implantation of D or He ions was carried out by using a ion gun with magnetically analyzed 10 keV D_2^+ ions or with 10 keV He^+ ions . The helium ion flux was $10^{13} cm^{-2} s^{-1}$ and deuterium ion flux was 10^{14} $cm^{-2} s^{-1}$. The implantation temperature was 300K and was monitored using a chromel-alumel thermocouple. Post-implantation annealing of specimens was performed in the temperature range 300-1200 K by resistance heating with a rate of 7 Ks^{-1}.

The substitution of deuterium for protium allows the use of nuclear reactions to determine the depth distribution and concentration of hydrogen isotopes. The irradiations and measurements by nuclear methods were performed in one chamber excluding contact of the specimens with the air. Contact of the specimens with the air may result in artefact trap sites associated with the surface oxide.

III. ANALYSIS OF THE RADIATION DAMAGE AND RANGE DISTRIBUTION PRODUCED BY INERT GASES AND HYDROGEN IMPLANTS

III.A. Profiles of deuterium and helium by means of nuclear reaction

III.A.1. Forward geometry

The implanted particle depth distribution was measured using the nuclear reactions $^3He(D,p)^4He$ and D $(^3He,p)^4He$. These measurements were performed using forward and back scattering geometry.

In forward geometry a beam of either ^3He or D_2 ions was incident at an angle of 30^o to the specimen surface and the nuclear reaction products were recorded at an angle of 60^0 with respect to the analyzing beam. The beam diameter during irradiation was 4 mm and during analysis was 2 mm (Fig. 2). The depth resolution in forward scattering geometry was determined to be ~15 nm.

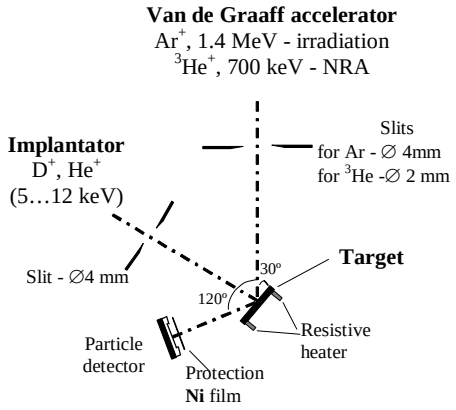

Fig. 2. Schematic drawing of experimental setup.

The implanted particle depth distribution was measured using the nuclear reactions ^3He $(D,p)^4He$ and D $(^3He,p)^4He$ with analyzing beams of D_2 (E = 1 MeV) and ^3He (E = 700 keV), respectively. The sensitivity of Nuclear Reaction Analysis method (NRA) is deteriorated by the presence of large sources of background. The main sources which interfere with the α and p signals (the reaction products) are pulse pileup from high rates of backscattered deuterons, high energy protons emitted from $^3He(d,p)^4He$ and $D(^3He,p)^4He$ and particles emitted from nuclear reactions of light elements in the targets, such as carbon, nitrogen or oxygen. All these interference sources distorted an energy spectrum of the reaction products. To determine the true depth profile, the experimental spectrum is fitted by using the GANRA program, in which the nuclear reaction cross-section and the stopping power of Ziegler are integrated.

Experimentally measured spectrums were approximated by set of Gaussians from layers with concentrations which were adjusted by using the special least square with regularization method (designed by Tichonov) which is commonly applied for solving non correct problems (Fig. 3).

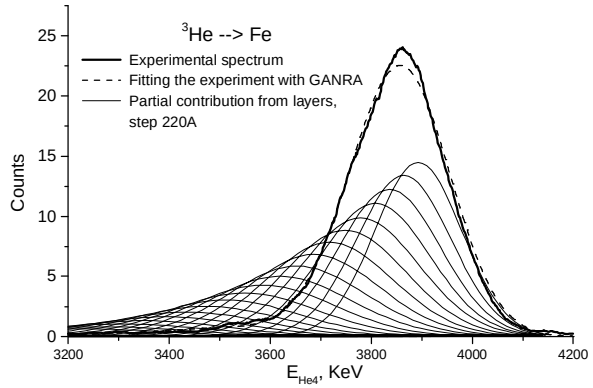

Fig. 3. Approximation of experimentally measured spectra by Gaussian set from uniform layers with different concentration of deuterium atoms.

For calibration of methodology the deuterium depth profile in aluminium obtained from the measured α yields by deconvolution with the program GANRA. It is in good agreement with SRIM 2006 calculations [4] (Fig. 4).

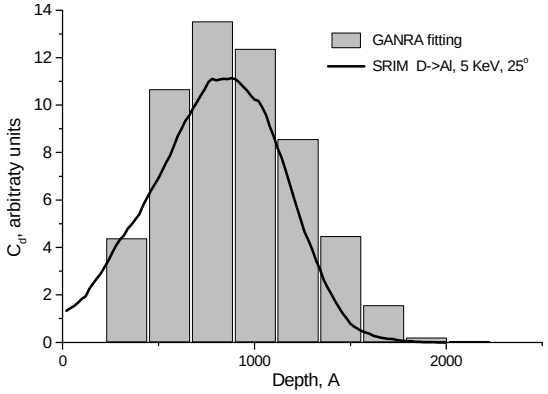

Fig. 4. Depth profile of deuterium concentration in the aluminum obtained from the measured α yields by deconvolution with the program GANRA. Calculated range distribution (SRIM) was plotted as solid line.

Fig. 5 shows deuterium distribution profiles in 18Cr10NiTi steel irradiated with 5 keV D^+ to $1 \cdot 10^{16}$ cm^{-2} at room temperature. The 18Cr10NiTi steel is used in states of the Former Soviet Union for nuclear applications where AISI 304 would be used in Western countries. Its composition is similar to AISI 321.

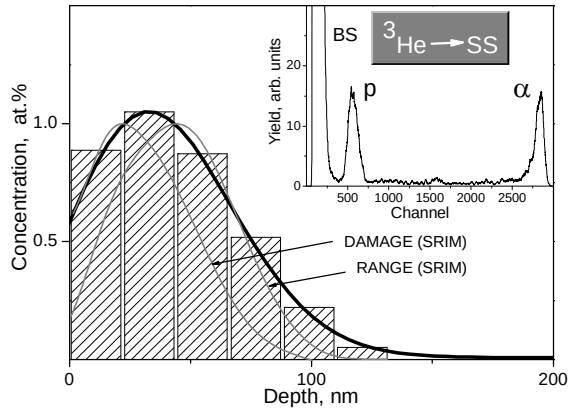

Fig. 5. Calculated and experimentally measured profiles of deuterium distribution in steel 08Cr18Ni10Ti after irradiation at T_{room}. Spectra of particles from nuclear reaction D(^{3}He,p)^{4}He are presented in the inserts on the figures.

Distribution profile of deuterium has the smeared peak and distribution width ~800 Å. The amount of deuterium contained in specimen under T_{room} constitutes ~80% respectively the irradiation dose (for spectrum set up ~15 min after irradiation termination). Experimentally measured profile correlates unsatisfactory with profiles calculated with SRIM program. The broadening of depth distribution and mismatch of profile maximum are due to the high mobility deuterium in stainless steel and as result its redistribution between ion range and damage profiles.

III.A.II. Backscattering geometry

In some cases, we are interested in profiling to greater depths. This was accomplished by backscattering geometry of NRA. The back-scattering of protons from D (^{3}He,p)^{4}He reaction was measured by surface-barrier detector tilted 157° to incident beam. Energy spectra of protons Y(E) were measured in the range of energies 0.3-1.6 MeV. Measurements were carried out by silicon semiconductor detector with the thickness of depleted zone ≈ 100 μm and $\Omega = 6.8 \cdot 10^{-4}$ st. To eliminate the registration of back scattered particles and to moderate the protons for their complete stopping in detector the aluminium foil with thickness 0.9 mm was placed before detector. On proton registration and on spectra processing the singularity of nuclear reaction D(^{3}He,p)^{4}He kinematics were taken into account, particularly that energy of protons emitted from reaction increases on decreasing the energy of ^{3}He in the target with deceleration.

For all range of energies of bombarding particles ^{3}He 0.3-1.6 MeV spectra of protons from reaction D(^{3}He,p)^{4}He and integral yields were determined. Fig. 6 shows as example the experimentally obtained energetic

dependence of integral yields of protons (markers*) and computed one by program Helen [5]. Program Helen realizes algorithm of A.N. Tikhonov regularization of incorrect problems in conformity with given equation (1) and operates with non-modified cross-section of reaction $D(^3He,p)^4He$. In the program the possibility of automatic and visual selection of regularization parameter is provided.

$$N_{He}\Omega \cdot \int_0^{r(E)} \sigma[Er(r(E)-x)] \cdot C(x)dx = Y(E), \quad (1)$$

where N_{He} – total number of incident ions ^3He with energy E; σ(E)-cross section of reaction; r(E)-projected path of ions $^3He^+$ in material; Er(r)-inverse function, Ω-solid angle.

Solid curve (marker-black rhombus) represents the protons yield Y(E) calculated from determined concentration ***C(x)*** (x-depth). The degree of curve deviation from experimental data (*) may serve as characteristic of calculated dependence C(x) truth.

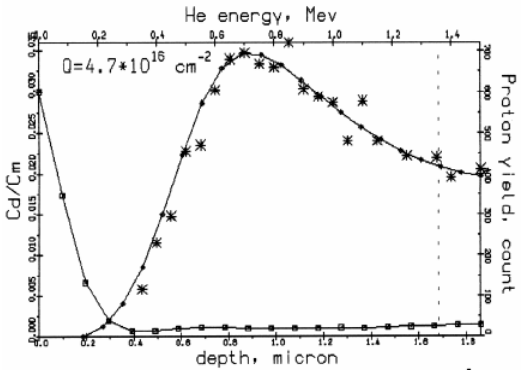

Fig. 6. Energy dependence of integral yields of protons (*) and distribution of deuterium in specimen of steel 18Cr10NiTi implanted with 20 keV D_2^+ ions (□) at T_{room} and annealing at 600 K. C_d, C_m-concentration of deuterium and host material, respectively. Note the concentration ~0.001 at.D/at.SS at large depth.

III.B. Analysis of lattice distortion by dechanneling

For DT fusion neutrons with the energy of 14 MeV, typical primary recoil atom energy for medium heavy target materials is around 400…1000 keV. The subject of this study was the number, type and depth distribution of defects produced in Ni under irradiation with ion beams He^+, Ar^+, Kr^+, Xe^+ with energy 0.2-1 MeV. The lattice distortion is investigated in the range of irradiation doses $1\cdot10^{15} – 2\cdot10^{17}cm^{-2}$. For each of three directions (<110>, <100>, <111>) the energy dependence yield of back scattered helium ions is obtained (backscattering spectra). The transfer from channel number on backscattering spectra to the scale of energies was carried out using of calibration curve for pulses analyzer. The common feature practically for all spectra measured in conditions of axial channeling is the presence of peaks in near-surface area and several times increase of backscattering yield in comparison with initial non-irradiated crystal (see Fig.7).

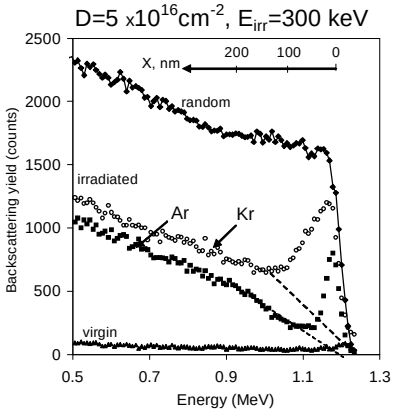

Fig. 7. Backscattering energy spectra (random and axial) of He^+ ions with energy 1.6 MeV in Ni <110> crystal in initial and Kr^+ and Ar^+ ions implanted at room temperature.

Peaks are produced by wide-angle scattering of He^+ ions on nickel atoms displaced from lattice sites. Fig. 8 shows the concentration depth distribution of scattering (displaced) atoms produced in Ni by irradiation with 300 keV Kr ions up to the doses $1\cdot10^{16}$ - $13\cdot10^{16}$ cm^{-2} under the room temperature.

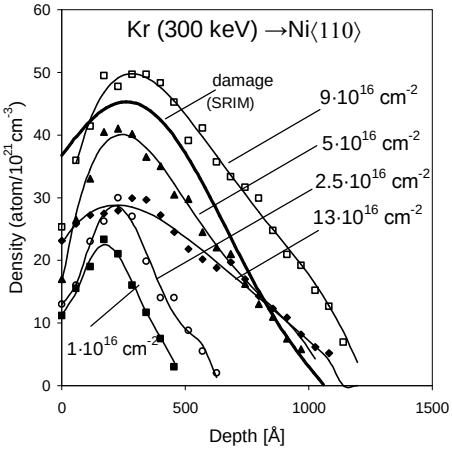

Fig. 8. Profiles of displaced atoms produced in Ni by irradiation with ions of krypton with energy 300 keV up to the doses $1\cdot10^{16}$…$13\cdot10^{16}cm^{-2}$ under the room temperature.

As it was noted the large dechanneled yield beyond the peak could be attributed to the multiple scattering by the extended defects, which accompany the extensive distortion lattice around the defects. In [6] is presented

the methodology of computation of spectra of backscattering channeled ions to obtain the information about the quantity and depth distribution of defects. From experimental axial and random spectra one can obtain the data on the normalized yield of backscattering for damaged (χ_d) and virgin (χ_v) crystals and plot the dependence of dechanneling parameter F_d=-ln[1-χ_d(t)]/[1-χ_v(t)] on depth.

The dechanneling yields of a backscattering spectrum for the inert gases implanted crystal can be relate to the number of defects in the path of the incident ions as follows [6]:

$$-\ln\left(\frac{1-\chi_d(t)}{1-\chi_v(t)}\right) = \lambda\int_0^t n(t')dt' \qquad (2),$$

where λ is the dechanneling cross-section for the defect and n(t) is the density of defects on the depth t.

Differentiating the equation (2) we obtain the depth distribution of defects causing the lattice distortion. Using this procedure for backscattering spectra we can determine the depth of damaged layer.

Fig. 9 presents the experimental data on normalized yield RBS (dechanneled yield) for virgin crystal of nickel (χ_v) and irradiated by helium ions with energy 200 keV (χ_d). The yield of RBS on depth up to 1 μm for irradiated crystal increases by one order in comparison with virgin specimen. On depth exceeding 1 μm dependencies χ_v(t) and χ_d(t) are parallel one to another ; it means the absence of radiation damage on this depth.

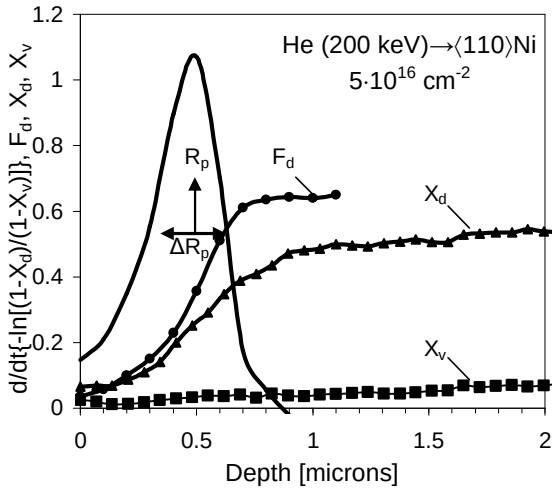

Fig. 9. Dependence of dechanneled yields for virgin crystal of nickel (χ_v) and irradiated by helium ions with energy 200 keV (χ_d), parameter of dechanneling (F_d) on depth and profile of damage. The mean (R_p) and FWHM (ΔR_p) for the SRIM range profile are shown.

Fig. 9 shows the dechanneling parameter (F_d) calculated on the base of experimental data and damage profile determined by differentiating the dependence F_d = f(t). The damage profile consists well with the depth profiles for helium ions with energy 200 keV in nickel calculated by SRIM-code. In this case protons with energy 1.4 MeV were used as analyzing ions; the specimen was analyzed on depth up to 6 μm.

In the case of argon ions irradiation as under irradiation by helium ions with energy 200 keV profile of damage coincides with calculated range distribution. But in the case of argon the damage on depth R_p +ΔR_p doesn`t decreases to zero; there is some degree of damage that extends to the depth several times exceeding projected range plus range spread (fig. 10).

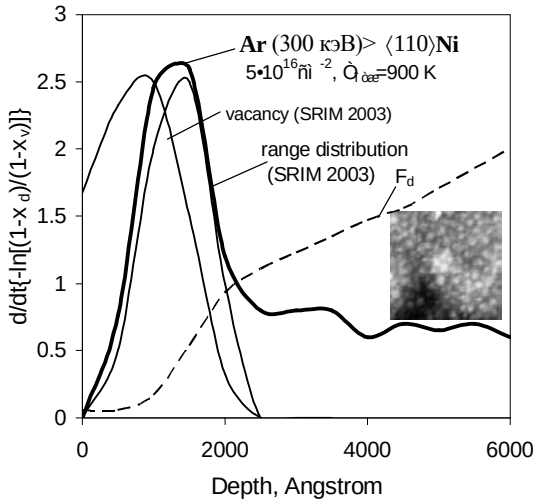

Fig. 10. Experimental and computed by program SRIM damage profile in nickel (vacancies and range distribution) for argon ions with energy 300 keV.

Electron-microscopic study of specimens irradiated by argon ions up to the dose $5\cdot10^{16}$cm^{-2} and annealed at temperature 900 K have shown the formation of gas bubbles (see insert on the figure 10). On annealing of specimens irradiated by krypton ions with energy 900 keV gas bubbles are also observed. But the long-range interaction is not observed. In the same time the damage profiles produced in nickel under krypton ion irradiation with energy 300 keV have “the tail” in distribution. The possible reason of observed particularities may be the difference in the processes proceeding in cascades produced by particles with different mass and energy. The heavy particles of argon and krypton with energy 300 keV as well as xenon with energy 630 keV produce cascades with high emission of energy that causes the damage of crystal structure on depth exceeding the range.

Fig. 11 presents the distribution profiles of xenon implanted into nickel with energy 630 keV (T_{irr}~300 K) up to the dose $2.5\cdot10^{15}$-$2.5\cdot10^{16}$cm^{-2}.

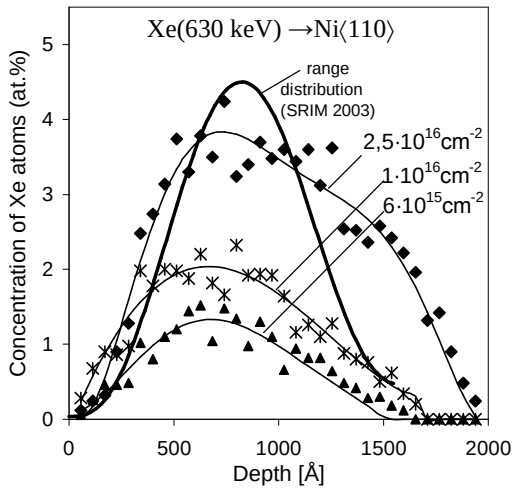

Fig. 11. Concentration depth profiles of xenon atoms implanted in nickel with energy 630 keV: experimental ones for irradiation dose $(0.6\text{-}2.5)\cdot10^{15}$cm^{-2} and computed by program SRIM 2003 profile of range distribution.

Comparison of experimental and computed distribution profiles of xenon atoms have show the coincidence of maximum location and the discrepancy of profile shape. This effect depends on dose. At $1\cdot10^{15}$ cm^{-2} the computed and experimental profiles coincide but at $3\cdot10^{15}$cm^{-2} the asymmetry occurs and increases with the irradiation dose. The observed variations indicate that with irradiation dose increase the redistribution of higher fraction of implanted xenon atoms in specimen on distance exceeding the range of Xe^+ ions (E=630 keV) in nickel. Irradiation by Xe^+ ions is carried out by tilting the specimen to axial channel to avoid the effect of channeling during implantation.

The position of Xe atom in Ni lattice is investigated up to the irradiation dose $1\cdot10^{15}$-$1\cdot10^{16}$cm^{-2}. The angular dependence of RBS yield was determined. It was established that the fraction of Xe atoms in regular substitutional position in Ni lattice (substitution fraction f_s) depends on irradiation dose. Under the irradiation dose of Xe^+ ions $1\cdot10^{15}$cm^{-2} f_s equals ~0.5 and for Kr ions in Ni (dose=$5\cdot10^{15}$cm^{-2}) $f_s \approx 0.8$, respectively. For irradiation doses $\geq1\cdot10^{16}$ cm^{-2} substitution fraction approaches zero.

The decrease of substitution fraction can be associated with formation of complexes xenon-vacancy. Concentration of different xenon-vacancy complexes causing experimentally observed angular dependencies were determined on the base of comparison of experimental and theoretically calculated orientation dependencies.

Fig. 12 shows the experimental and calculated angular dependencies of backscattering yield of Ni and Xe atoms. The best fitting of experimental and calculated values of angular dependencies was obtained when under the irradiation dose equal $3\cdot10^{15}$cm^{-2} 85% of Xe atoms are in the complexes Xe+v, 15% - in complexes Xe+2v. Under the dose of $6\cdot10^{15}$cm^{-2} 60% of Xe atoms form the complexes Xe+2v.

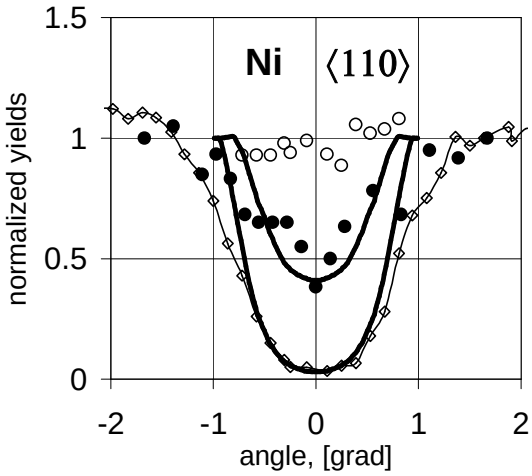

Fig. 12. Experimental (◊ - Ni, o, • -Xe) and calculated (solid line) angular dependencies of backscattering yield on scanning in axis <110>, • - dose $3\cdot10^{15}$cm^{-2}, o - $1\cdot10^{16}$cm^{-2}.

It should be noted that Xe-vacancy complexes are not split, because neither experimental data nor results of mathematical simulation don`t demonstrate stable complexes with atoms of Xe in interstitial position. In the same time as it follows from paper [7] splitted vacancy complex consists of 2 vacancies and impurity of high radius in interstitial position (so called centers of recombination of variable polarity) were revealed in system NiSc. The mechanisms of their nucleation and the effect of such centers on radiation stability of materials were proposed [7]. It was supposed that the main role in such complexes nucleation is played by dimension factor. On the base of results obtained in this paper we can state that apart the dimension factor the chemical bond (interatomic potential) play the important role in the process of splitted complexes nucleation.

III.D. High Energy Primary Knock-on Process in Metal-deuterium Systems by Bombardment with Noble Gas Ions

An experimental study confirms the possibility of initiating nuclear fusion reactions in metal-deuterium targets by bombarding them with ions that are not the reagents of the fusion reaction, in particular, with noble gas ions [8]. When energetic heavy ions irradiate a metal-deuterium target, a number of recoil deuterium atoms are produced in the solid. The recoil deuterium atoms cause

deuteron-deuteron (*d*,*d*) fusion reactions in solids. The evidence of fusion reactions was given by emission of tritium (E=1.05 MeV), protons (3.02 MeV), alpha particles (3.52 MeV for metal-deuterium+tritium systems) and neutrons. The yields of (*d*,*d*) and (*d*,*t*) reactions were determined as functions of energy (0,4 to 3.2 MeV) and mass of incident ions (He^+, Ne^+, Ar^+, Kr^+ and Xe^+). In experiments we used the titanium films prepared by deposition in an ultrahigh vacuum onto nickel or molybdenum and then saturated with pure deuterium or a tritium. Targets with a deuterium-tritium mixture were prepared by implanting 20-keV D_2^+ ions into a 0.6-μm-thick titanium+tritium film. The deuterium concentration and depth distribution in the films was measured by nuclear reaction $D(^3He,p)\alpha$ analysis.

We measured the yields from (*d*,*d*), (*d*,*t*) and (*t*.*t*) reactions as functions of incident ion energy for each type of ion studied. The yields were defined as the number of reaction events occurring in the given target per incident ion. Figs. 13 and 14 show plots of proton and alpha particles yields, respectively, resulting from the bombardment of the targets containing the deuterium and deuterium-tritium mixture by He^+, Ne^+, Ar^{2+}, Kr^{2+} and Xe^{2+} ions as functions of incident ion energy. Open circles, triangles and squares in Figs. 13, 14 are experimental data. The features of energy dependence of yields are the practically linearly grow of proton yields (Fig. 13) and decrease in the rate of alpha-particle yields (Fig. 14) when R_p of incident ions become equal the target thickness [8].

The theory of nuclear fusion reactions in atomic collision cascades initiating by noble gas ion beam in metal-deuterium target is developed. The method for calculating tritium or deuterium recoil fluxes and the yield of d-d fusion reaction in subsequent collisions was proposed. It is supposed that the collisions of moving isotopes of hydrogen with immobile partners cause the excitation of reactions of nuclear synthesis. It is possible to calculate the energy distribution of the recoil atoms, if the energy dependence of the cross section for the reaction is known. The probability of d-d fusion reaction has been calculated for primary colliding deuterium atoms. Each component of moving atoms flow is characterized by its own function of distribution by energies that extend from zero to maximum energy of PKA of corresponding type. Using Molier potential for description of atomic interaction we obtained the equation for the yield (d, d) from the depth of target *x* with deuterium concentration n_D. Numerical results of simulations shown as solid lines in Figs. 13, 14.

Fig. 15 represents the spectral density of yield nuclear reaction at different depths in the target TiD_2. Fig.16 shows the theoretical dependence of deuterium knocked-out atoms energy spectrum in the target bombardment with 3.2 MeV Kr^+ ions.

As seen in Figs. 15, 16 the main contribution into the yield of reaction of synthesis (on all depths) gives the deuterium atoms with energies that are considerably lower than maximal energies of PKA $T_{max}(x)$ on given depth.

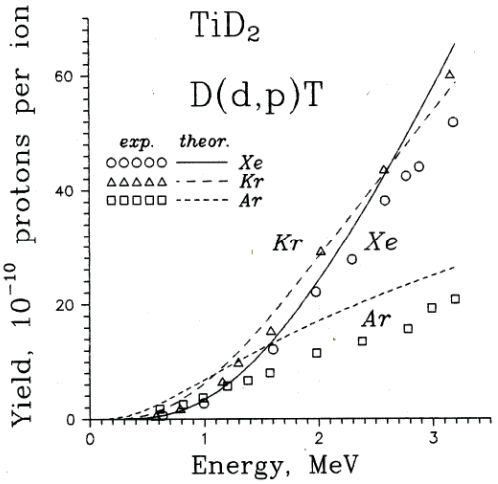

Fig. 13. Dependence of proton yields from TiD_2 target on noble gas ion energy. Points show experimental values, lines – calculation results.

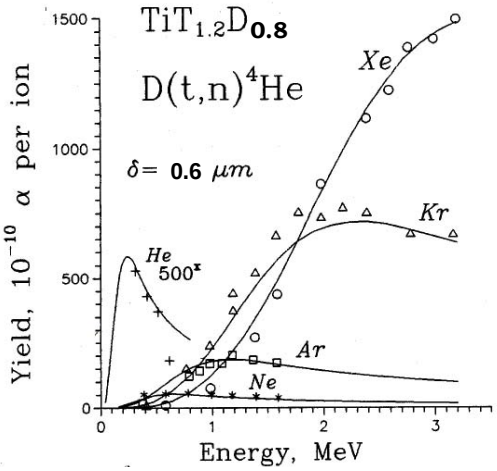

Fig. 14. Energy dependences of alpha-particle yields from the $d(t,n)^4He$ reaction occurring in the $TiT_{1.2}D_{0.8}$ target under ion bombardment. Points - measured values, lines – calculated results.

The following conclusions have been obtained: the nuclear reactions of D(d,p)t and $D(t,n)^4He$ mainly occur in energy region of the recoiled D-atom from 5 keV to 125 keV. This means that excitation of nuclear synthesis reaction proceeds in collision cascades as deceleration of primary knocked-out atoms of deuterium in the target. The contribution of low-energetic atoms in complete yield is predominant in spite of sharp decrease of cross section

of reactions in the range of low energies. Teshigawara et al. [9] reported that the nuclear reactions of D(d,p)t mainly occur in the energy of the recoiled D-atom from 10 keV to 100 keV.

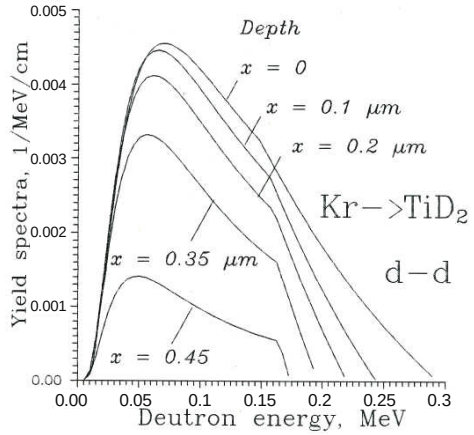

Fig. 15. Theoretical energy dependence of the spectral density of yield nuclear reaction d(d,p)T at different depths in the target TiD_2 bombardment with 3.2 MeV Kr^+ ions.

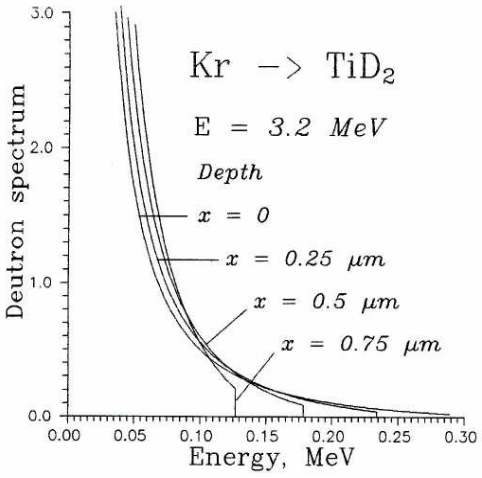

Fig. 16. Theoretical dependence of the deuterium knocked-out atom energy spectrum in TiD_2 target under 3.2 MeV Kr^+ bombardment ions.

The obtained experimental results are well described in the model of excitation of nuclear reactions of synthesis in cascades of atomic collisions initiated by external irradiation of hydrogen containing materials. It supposes the possibility of use of nuclear synthesis reactions excitation as unique method of investigation of atom-atomic collisions cascades allowing to the information on cascade functions, distribution of particles by energies and other characteristic of cascade processes in multi component materials.

IV. CONCLUSIONS

The accelerators and ion beam analysis techniques are useful for the simulation of displacement damage and detailed investigation of distribution profiles of damage and impurity atoms under irradiation of targets in wide range of doses and energies of particles. Charged particle-materials interaction research may produce very important information for nuclear materials R & D.

REFERENCES

1. F. A. GARNER, E. P. SIMONEN, B. M. OLIVER, L. R. GREENWOOD, M. L. GROSSBECK, W. G. WOLFER and P. M. SCOTT, "Retention of Hydrogen in FCC Metals Irradiated at Temperatures Leading to High Densities of Bubbles or Voids", *Journal of Nuclear Materials*, **356**, 122 (2006).
2. G. D. TOLSTOLUTSKAYA, V. V. RUZHYTSKIY, I. E. KOPANETS, S. A. KARPOV, V.V. BRYK, V. N. VOYEVODIN, F. A. GARNER, "Displacement and Helium-Induced Enhancement of Hydrogen and Deuterium Retention in Ion-Irradiated 18Cr10NiTi Stainless Steel", *Journal of Nuclear Materials*, **356**, 136 (2006).
3. S. NAGATA, K. TAKAHIRO, "Deuterium Retention in Tungsten and Molybdenum", *Journal of Nuclear Materials*, **283-287**, 1038 (2000).
4. www.srim.org.
5. I. ZHUKOV, G. D. TOLSTOLUTSKAYA, V. F. RYBALKO, I. E. KOPANETS, L. F. VERKHOROBIN, "Determination of Deuterium Depth Profiles in Materials from Nuclear Reaction Product Yields", *Questions of Atomic Science and Techniques (VANT) in Series: "Physics of Radiation Damage and Radiation Material Science"*, **1(58)** and **2(59)**, 133 (1992) (in Russian).
6. S. T. PICRAUX, D.M.FOLLSTAEDT, P. BAERI, S. U. CAMPISANO. G. FOTI, E. RIMINI, "Depth Profile Studies of Extended Defects Induced by Ion Implantation in Si and Al", *Radiation Effects*, **49**, 75 (1980).
7. A. S. BAKAY, V. F. ZELENSKY, I. M. NEKLYUDOV, "Centers of Point Defects Recombination of Variable Polarity", *JTPh.*, **57**, 2371 (1987) (in Russian).
8. V. F. ZELENSKY, V. F. RYBALKO, G. D. TOLSTOLUTSKAYA, S. V. PISTRYAK, I. E. KOPANETS, A. N. MOROZOV, "Initiation of Nuclear Fusion Reactions in Metal-Deuterium and Metal-Deuterium+Tritium Systems by Bombardment With Noble Gas Ions", *Fusion Technology*, **25**, 95 (1994).
9. M. TESHIGAWARA, K.KONASHI, H.KAYANO, "Measurement of a knock-onprocess induced by an ion beam", *Journal of Nuclear Materials*, **248**, 439 (1997).